

## Growth and Characterization of Langasite-type Single Crystals Substituted with Aluminum to the Solubility Limit

Hiroaki Takeda, Satoshi Tanaka, Tadashi Nishida,  
Kiyoshi Uchiyama and Tadashi Shiosaki

Graduate School of Materials Science, Nara Institute of Science and Technology (NAIST),  
Takayama-cho 8916-5, Ikoma, Nara 630-0192, Japan  
Fax: +81-743-72-6069, e-mail: hiro-t@ms.naist.jp

We describe the process to grow the aluminum-substituted langasite-type,  $\text{La}_3\text{Ta}_{0.5}\text{Ga}_{5.5-x}\text{Al}_x\text{O}_{14}$  (LTGA $x$ ), single crystals with a uniform Al concentration by the conventional Czochralski technique. The solid-state reaction of the raw material powders was performed for an investigation of the Al substitution limit. The results showed that the LTGA $x$  polycrystals have the wide solid-solution range of  $0 \leq x \leq 2.0$ . The LTGA $x$  single crystals with  $0 \leq x \leq 1.0$  were grown on the basis of the pseudo binary phase diagram, where one of the end members is the pure  $\text{La}_3\text{Ta}_{0.5}\text{Ga}_{5.5}\text{O}_{14}$  (LTG) phase. The Al content  $x$  in these LTGA $x$  single crystals decreases with the growth process. In this study, we obtained LTGA $x$  single crystals up to  $x=0.5$  without any inclusions, but with a small change in the chemical composition. The piezoelectric moduli  $d_{11}$  and  $d_{14}$  values of the LTGA0.5 crystals are greater than those of the pure LTG ones.

*Key words:* phase diagram, crystal growth, solid-solution, solubility limit, piezoelectric property

### 1. INTRODUCTION

Recently, piezoelectric materials for high temperature use are strongly demanded for gas sensors, and for combustion pressure sensors and gas injectors directly placed in the cylinder of engines. The candidates for the sensor material are AlN thick films [1],  $\text{GaPO}_4$  crystals [2], and  $\text{La}_3\text{Ga}_5\text{SiO}_{14}$  (langasite, LGS) crystals [3]. Among them, we have paid attention to the LGS single crystals, because LGS shows no phase transitions up to its melting temperature and can be easily grown to a large size using the Czochralski (Cz) technique [4-6]. For practical use, the LGS crystals need both a low temperature dependence of the piezoelectric properties and a high electric resistivity  $\rho$  at high temperature for real applications. Unfortunately, the LGS crystals grown in a conventional oxygen-containing atmosphere have a low  $\rho$  value ( $4.0\text{E}+8 \text{ }\Omega\text{cm}$ ) at high temperature ( $400^\circ\text{C}$ ). The desired  $\rho$  value is greater than  $1\text{E}+9 \text{ }\Omega\text{cm}$  at  $400^\circ\text{C}$  for practical use. Very recently, Taishi *et al.* [7] successfully improved the resistivity of the LGS crystals. The crystals were grown in inert gasses ( $\text{N}_2$  or Ar), and the  $\rho$  value was  $10\text{-}10^2$  times higher than that of the LGS crystals grown in the oxygen-containing atmosphere. We have found another way to increase the electric resistivity of the LGS crystals. By substituting  $\text{Al}^{3+}$  ions for some of the  $\text{Ga}^{3+}$  ones, we obtained the LGS crystals with a higher electric resistivity [8]. This substitution should be applied to other LGS-type crystals.

Up to now, more than 140 LGS-type crystals have been synthesized [9-12]. However, little is known about the piezoelectric properties of these LGS-type crystals over  $200^\circ\text{C}$ . Therefore, it has not been clarified that LGS is the most appropriate material of all the LGS-type crystals. Under this condition, an isomorphous  $\text{La}_3\text{Ta}_{0.5}\text{Ga}_{5.5}\text{O}_{14}$  (LTG) single crystal is a very attractive material. The LTG single crystals can be grown by the

Cz technique [13,14], and exhibit a higher frequency stability and high electromechanical coupling factors compared with the LGS one [13,15]. The LTG crystal congruently melts [14], whereas the LGS is a peritectic phase [16,17]. These results showed that LTG is a more suitable material for the mass production of piezoelectric devices with a more uniform quality than LGS. Moreover, in the temperature range of  $-50\text{-}80^\circ\text{C}$ , the LTG crystals show a low temperature dependence of the piezoelectric properties compared to LGS [15]. Therefore, we believe that the LTG single crystal is a promising candidate as a combustion pressure sensor material.

We have already grown and characterized the Al-substituted LTG,  $\text{La}_3\text{Ta}_{0.5}\text{Ga}_{5.5-x}\text{Al}_x\text{O}_{14}$  (LTGA $x$ ) single crystals [8]. The crystals showed an improvement in the resistivity similar to the LGS. In ref. [8], the substitution effect of  $\text{Al}^{3+}$  for  $\text{Ga}^{3+}$  in LTG on the electric properties was mainly reported. In this paper, we focus on the influence of the Al substitution on the growth process of the LTG single crystals. We also report the material constants of the LTGA $x$  crystals compared to those of the pure LTG one.

### 2. EXPERIMENTAL

Before growth of the LTGA $x$  crystals, the solubility limit of Al into LTG was investigated by the solid state reaction and powder X-ray diffraction analysis. For the solid state reaction, a total of 12 mixtures of LTGA $x$  ( $x=0.0\text{-}5.5$  at intervals of 0.5) were prepared. A platinum sheet ( $100 \times 100 \text{ mm}^2$ ) containing each pellet-like mixture was placed in an electric furnace and stepwise heated in increments of  $20^\circ\text{C}$ . In the temperature range near the melting point, after heating, the samples were removed from the furnace. The cooled samples were pulverized, and a phase identification was

performed by X-ray powder diffraction.

On the basis of the determined diagram, the single crystals of LTGA $x$  were grown from the starting melt compositions with various Al content by the Cz technique. Single crystals were grown by the conventional RF-heating Cz technique using an iridium crucible (40-50 mm diameter and height). The starting materials were prepared by mixing 99.99% pure La $_2$ O $_3$ , Ta $_2$ O $_5$ , Ga $_2$ O $_3$  and Al $_2$ O $_3$  powders. The powders were mixed in air, and then calcined at 1000°C for 2 h. They were then heated at 1350 °C for 5 h. The calcined powders were charged into the crucible. The growth atmosphere was a 1 vol%O $_2$ +Ar gas flow at 10 $^{-3}$  m $^3$ /min. The pulling rate and the rotation rate were 1.5 mm/h and 15-20 rpm, respectively. The observation of bubbles and inclusions in the crystals was performed using an optical microscope. The phase identification of these crystals was performed by the X-ray diffraction (XRD) technique. The density of the grown crystals was measured by Archimedes method using distilled water at room temperature. The substitution effect on the crystal quality was examined by measuring the chemical composition. The chemical composition of the crystals was measured by a quantitative X-ray fluorescence analysis.

Langasite-type crystals belong to the trigonal system P321. The independent material constants in point group 32 consist of two dielectric, two piezoelectric and six elastic compliance constants ( $\epsilon_{ij}$ ,  $d_{ij}$  and  $s_{ij}$ , respectively). The material constants of LTG and LTGA0.5 were determined using an impedance/gain phase analyzer (HP 4194A: Agilent) as reported in refs.[18,19]. The electromechanical coupling factor  $k_{ij}$  and the piezoelectric modulus were evaluated by measuring the mechanical series resonance frequency  $f_s$  and parallel resonance frequency  $f_p$  of the equivalent resonators. The equivalent resonators were fabricated in the form of plates according to the length-extensional vibration mode. The dielectric constants  $\epsilon_{ij}$  were determined by measuring the capacitances of the resonators by taking the parasitic capacitance into account.

### 3. RESULTS AND DISCUSSION

#### 3.1 Growth concept of Al-substituted crystals

In earlier studies [20-22], the authors reported the substitution effects of Ga $^{3+}$  in LGS by Al $^{3+}$  on the crystal growth and piezoelectric properties. The chemical formula is La $_3$ Ga $_{5-x}$ Al $_x$ SiO $_{14}$  (LGAS $x$ ). A part of the crystal structure is schematically shown in Fig. 1. In the langasite structure, there are four kinds of cation sites in the structure with the chemical formula  $A_3BC_3D_2O_{14}$ . The notations  $A$  and  $B$  represent a decahedral (twisted Thomson cube) site coordinated by eight oxygens, and an octahedral site coordinated by six oxygens, respectively. Moreover,  $C$  and  $D$  represent the tetrahedral sites coordinated by four oxygens; the size of the  $D$  site is smaller than that of the  $C$  site. In the LGS crystal, La $^{3+}$  occupies the  $A$  site, Ga $^{3+}$  occupies the  $B$ ,  $C$  and half of the  $D$  sites, and Si $^{4+}$  occupies half of the  $D$  sites. In the LGAS $x$  crystals, the Al atoms are distributed in all the cation sites ( $B$ ,  $C$  and  $D$ ) except for the  $A$  one by rather favoring the smallest  $D$  one [22]. In refs.[20,21], the authors reported that: (1) the LGAS $x$  crystal has the Al solubility limit ( $x < 1.0$ ), (2) the

effective segregation coefficient  $k_{\text{eff}}$  of Al in LGS is between 1.03 and 1.07, and (3) the perovskite-type La(Al,Ga)O $_3$  phase occurred in the LGAS1.0 crystal. On the basis of these observations, we can draw the phase diagram of a pseudo binary system of LGS-La $_3$ Al $_5$ SiO $_{14}$  as shown in Fig. 2. In this diagram, for visual convenience, we adopted La $_3$ Al $_5$ SiO $_{14}$  which is a hypothetical complex oxide. This diagram shows the presence of a solid solution without a maximum or minimum at  $x < 1.0$  and the LGAS $x$  crystals with a continuously changing composition such as the Si-Ge alloy [23]. For a crystal forming solid solution, it is generally difficult to control the crystal uniformity and ensure the reproducibility of the physical and chemical properties. However, as seen in Fig.2, we have an opportunity to develop the process for the effective segregation coefficient  $k_{\text{eff}}$  of unity. When we find the Al solubility limit of the LGAS $x$  (of course, LTGA $x$ ) crystals, we can grow the crystal with a uniform composition.

#### 3.2 Phase diagram and Growth Phenomena

Fig.3 shows the phase change of the LTGA $x$  powders after the solid-state reaction versus the Al content  $x$ . This figure is considered to be the phase diagram of the

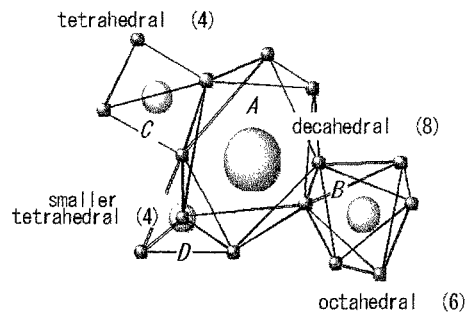


Fig.1 Schematic coordination polyhedra of oxygen atoms around cationic atoms in langasite-type structure. Small circles represent oxygen atoms

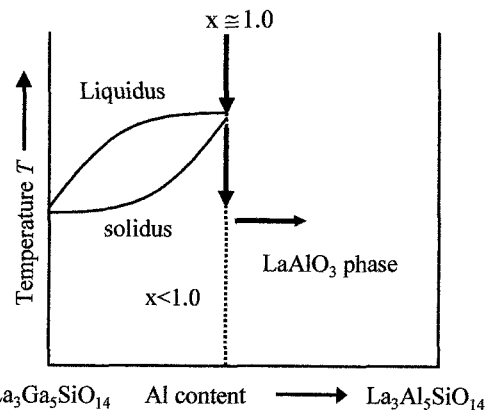


Fig.2 Hypothetical phase diagram of pseudo-binary system containing La $_3$ Ga $_5$ SiO $_{14}$  with Al doping. This diagram is based on the data reported in refs.[20-22].

pseudo binary system of LTG-La<sub>2</sub>Ta<sub>0.5</sub>Al<sub>5.5</sub>O<sub>14</sub> (LTA), which is a hypothetical complex oxide. The diagram shows that the LTGA<sub>x</sub> single phase is obtained up to  $x=2.0$  as the polycrystalline state, and that no LTGA<sub>x</sub> phases are obtained over  $x=3.0$ . The LTG melts around 1490°C [13]. We also found the effect of the Al content ( $x$ ) on the temperature of the melting point of the LTGA<sub>x</sub> samples. As seen in Fig.3, the melting temperature increased with change in the Al content. This result suggested that Al<sup>3+</sup> ions are easily incorporated into the crystals during the growth process, in other words, the segregation coefficient of Al is greater than unity. This result agreed with the melting behavior of the LGAS<sub>x</sub> single crystal [20]. In ref.[20], the authors also reported that the LGAS<sub>x</sub> single crystal without any imperfections was obtained up to  $x=0.9$ . The Al content in the single crystals is smaller than those ( $x=1.5$ ) in the polycrystalline state. Therefore, we must decrease the Al content in the starting melt composition for growing LTGA<sub>x</sub> crystals.

In this study, we first tried to grow the LTGA1.0 crystals, in which the Al content is half the Al solubility limit in the LTGA<sub>x</sub> polycrystal. We also grew a pure LTG single crystal at the same time for comparison (Fig. 4a). The pure grown LTG crystal had a 25-mm diameter and 130-mm length. By the way, the grown LTGA1.0 boule had a smooth surface, but was opaque with a light orange color. Many inclusions were observed inside the crystal. Therefore, we have grown LTGA<sub>x</sub> crystals from the starting material with incremental changes in the Al-content of 0.1. Fig. 4b shows an as-grown LTGA0.6 crystal. Although the uniform diameter of the grown crystals was easily controlled, the growth instability appeared during the growth below the tail part as indicated by the dotted line in Fig. 4. The crystals showed a smooth surface and were transparent with a orange color till the inclusions appeared. All peaks in the powder XRD patterns of the transparent part of the boule were identified to be those of the LTG-type structure. Finally, we obtained LTGA0.5 single crystals with no secondary phases as seen in the ref.[8]. Up to  $x=0.5$ , the LTGA<sub>x</sub> crystals were grown in the same way as the LTG one. Incidentally, the LTGA0.5 single crystal was grown using an Ir crucible with a 40 mm diameter and height. For the other crystals, an Ir crucible with 50 mm diameter and height was used. The measured density ( $D_m$ ) of the LTG and LTGA0.5 crystals was 6.138(4) and 5.99(1) g/cm<sup>3</sup>, respectively. (see Table 1). This result is supported by the difference in the atomic weight ( $W_{Al}(26.98) < W_{Ga}(69.72)$ ). Therefore, we confirmed the Al substitution into the LTG.

Fig. 5 shows the results of the chemical composition analysis along the growth direction of the LTGA<sub>x</sub> crystals with  $x=0.1$ , 0.5, and 0.6. In the figure,  $C_{int}$  and  $C_S$  represent the concentration of Al<sub>2</sub>O<sub>3</sub> at initial and each cylinder part of the boules, respectively. As can be seen, the concentration of Al<sub>2</sub>O<sub>3</sub> in the all crystals decreases with the crystal growth. This shows that the  $k_{eff}$  of this oxide was found to be over unity. This result agreed with the observation derived from the phase diagram shown in Fig. 3. Among the three crystals, LTGA0.5 has the smallest variation in the Al<sub>2</sub>O<sub>3</sub> concentration within the investigated composition in this

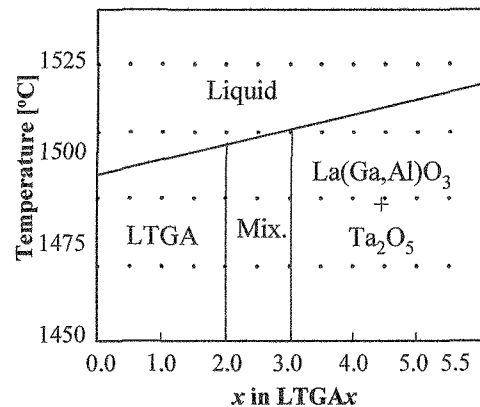


Fig. 3 Phase change of LTGA<sub>x</sub> powders after solid-state reaction versus the Al content  $x$ . The dots indicated the temperatures and the compositions where the reaction process was carried out. The "Mix." denotes the mixture of the LTGA, La(Ga,Al)O<sub>3</sub>, and Ta<sub>2</sub>O<sub>5</sub> phases.

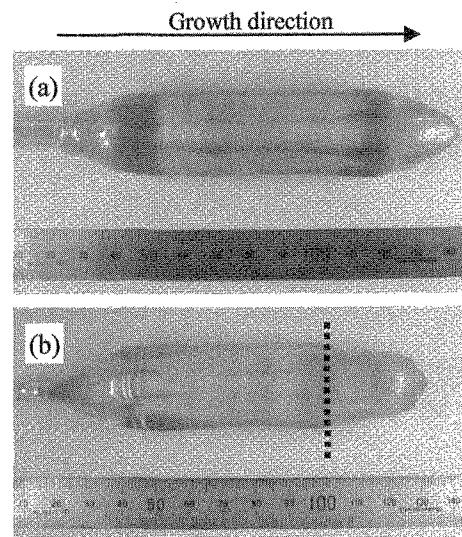


Fig. 4 As-grown (a) LTG and (b) LTGA0.6 crystals. Inclusions are observed in the part below the dotted line.

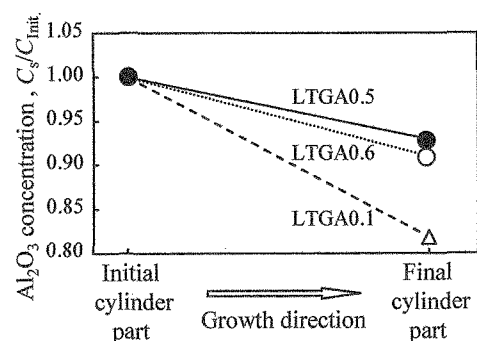


Fig. 5 Al<sub>2</sub>O<sub>3</sub> concentration change in the grown LTGA<sub>x</sub> crystals.

study. Hence, these results suggest that the starting melt composition of LTGA0.5 is closer to the composition which can produce a crystal with a uniform composition.

### 3.3 Aluminum substitution effect on piezoelectric properties

The electromechanical coupling factors and evaluated material constants of the LTG and LTGA0.5 single crystals are shown in Table 1. All the factors of the LTGA0.5 sample are greater than those of the pure LTG. This result is the same as that reported for the Al-substituted LGS crystals [20-22]. The LTGA0.5 crystal also has higher piezoelectric constants,  $d_{11}$  and  $d_{14}$ , as the absolute values compared with pure LTG crystal. In ref.[8], we reported the low temperature dependence of  $d_{11}$  of the LTGA0.5 crystals and the improvement of the electric resistivity by the Al substitution into the LTG crystals. In addition, in this paper, we mentioned that the Al substitution enables the use of a lower amount of expensive gallium oxide as the raw material. For the LTGA0.5 crystal, a reduction (approximately 9%) in the  $\text{Ga}_2\text{O}_3$  amount versus LTG is expected. Therefore, we can say that the LTGA0.5 crystal is the top-ranked candidate for combustion pressure sensor materials.

Table 1 Properties of LTGAx crystals.

	LTG	LTGA0.5
$D_m$	6.138	5.991
$k_{12}$	16.4	16.6
$k_{23}$	6.09	6.95
$\varepsilon_{11}^T/\varepsilon_0$	$20.0 \pm 0.3$	$19.7 \pm 0.3$
$\varepsilon_{33}^T/\varepsilon_0$	$79.9 \pm 0.2$	$67.9 \pm 0.1$
$d_{11}$	6.59	6.64
$d_{14}$	-3.68	-4.19
$s_{11}^E$	9.07	9.08
$s_{12}^E$	-4.51	-4.55
$s_{13}^E$	-1.95	-2.00
$s_{14}^E$	-3.54	-3.70
$s_{33}^E$	5.18	5.27
$s_{44}^E$	21.9	21.8
$s_{66}^E$	27.2	27.3

- $D_m$  : Experimental density [g/cm<sup>3</sup>]  
 $k_{ij}$  : Electromechanical coupling factor  
 $\varepsilon_{ij}^T/\varepsilon_0$  : Relative dielectric constant  
 $d_{ij}$  : Piezoelectric constant [pC/N]  
 $s_{11}^E$  : Elastic compliance constant [ $\times 10^{12}$  m<sup>2</sup>/N]

## 4. SUMMARY

We proposed a way to grow an LTGAx solid-solution crystal with a uniform composition. We constructed the phase diagram of the pseudo binary system of LTG-LTA by synthesis of the Al-substituted LTG (LTGAx) polycrystal. Subsequently, we grew LTGAx crystals by the conventional Cz technique. Although the crystal quality, i.e., uniform composition, is open to further improvement, at present, the LTGA0.5 single crystals with a small composition change were obtained. By Al-substitution, the LTG crystals acquired better

piezoelectric properties.

## ACKNOWLEDGEMENTS

This work was partly supported by a Grant-in-Aid for Young Scientists Research No. 17686058 from the Ministry of Education, Culture, Sports, Science and Technology of Japan and a research grant from The Mazda Foundation.

## REFERENCES

- [1] Y. Oishi, H. Noma, K. Kishi, N. Ueno, M. Akiyama and T. Kamohara, *J. Ceram. Soc. Jpn.* **113** (2005) 700. [in Japanese]
- [2] P. Kreml, G. Schleinzner and W. Wallnöfer, *Sens. Actuators A: Phys.* **61** (1997) 361.
- [3] H. Fritze and H. L. Tuller, *Appl. Phys. Lett.* **78** (2001) 976.
- [4] O. A. Buzanov, A. V. Naumov, V. V. Nechaev, S. N. Knyazev, *Proc. 1996 IEEE Inter. Freq. & Contr. Sym.* (1996) 131.
- [5] K. Shimamura, H. Takeda, T. Kohno and T. Fukuda, *J. Crystal Growth* **163** (1996) 388.
- [6] S. Uda, S. Q. Wang, N. Konishi, H. Inaba and J. Harada, *J. Cryst. Growth* **237-239** (2002) 707.
- [7] T. Taishi, K. Kato, T. Hayashi, K. Fujiwara, N. Banba, T. Fukami, K. Hoshikawa, *Proc. Piezoelectric Mater. & Device Sym. 2005* (2005) 21. [in Japanese].
- [8] H. Takeda, S. Tanaka, S. Izukawa, H. Shimizu, T. Nishida and T. Shiosaki, *Proc. 2005 IEEE Ultrasonics Symp.* (in press)
- [9] B. V. Mill, A. V. Butashin, G. G. Khodzhabyan, E. L. Belokoneva, N. V. Belov, *Sov. Phys. Dokl.* **27** (1982) 434.
- [10] B. V. Mill, A. V. Butashin, A. M. Éllern, *Inorg. Mater.* **19** (1984) 1516.
- [11] B. V. Mill, E. L. Belokoneva, T. Fukuda, *Russ. J. Inorg. Chem.* **43** (1998) 1032.
- [12] B. V. Mill, E. L. Belokoneva, T. Fukuda, *Russ. J. Inorg. Chem.* **43** (1998) 1168.
- [13] H. Kawanaka, H. Takeda, K. Shimamura and T. Fukuda, *J. Crystal Growth* **183** (1998) 274.
- [14] H. Takeda, H. Kawanaka, N. Onozato, T. Fukuda, *J. Mater. Sci. Mater. Electr.* **12** (2001) 199.
- [15] N. Onozato, M. Adachi and T. Karaki, *Jpn. J. Appl. Phys.* **39** (2000) 3028.
- [16] H. Takeda, K. Shimamura, V.I. Chani and T. Fukuda, *J. Crystal Growth* **197** (1999) 204.
- [17] S. -Q. Wang and S. Uda, *J. Cryst. Growth* **250** (2003) 463.
- [18] *IEEE Standard on Piezoelectricity* 176-1987 (1987).
- [19] W. P. Mason, "Piezoelectric crystals and their application to ultrasonics", New York, D. Van Nostrand Company, 1950.
- [20] M. Kumatoriya, H. Sato, J. Nakanishi, T. Fujii, M. Kadota and Y. Sakabe, *J. Cryst Growth* **229** (2001) 289.
- [21] H. Takeda, M. Kumatoriya and T. Shiosaki, *Key Eng. Mater.* **216** (2002) 43.
- [22] H. Takeda, M. Kumatoriya, T. Shiosaki, *Appl. Phys. Lett.* **79** (2001) 4201.
- [23] I. Yonenaga, *J. Cryst. Growth* **198-199** (1999) 404.